Stochastic resetting and the mean-field dynamics of focal adhesions

Paul C. Bressloff
Department of Mathematics, University of Utah Salt Lake City, Utah 84112, USA

(Received 20 May 2020; accepted 12 August 2020; published 24 August 2020)

In this paper we investigate the effects of diffusion on the dynamics of a single focal adhesion at the leading edge of a crawling cell by considering a simplified model of sliding friction. Using a mean-field approximation, we derive an effective single-particle system that can be interpreted as an overdamped Brownian particle with spatially dependent stochastic resetting. We then use renewal and path-integral methods from the theory of stochastic resetting to calculate the mean sliding velocity under the combined action of diffusion, active forces, viscous drag, and elastic forces generated by the adhesive bonds. Our analysis suggests that the inclusion of diffusion can sharpen the response to changes in the effective stiffness of the adhesion bonds. This is consistent with the hypothesis that force fluctuations could play a role in mechanosensing of the local microenvironment.

DOI: 10.1103/PhysRevE.102.022134

I. INTRODUCTION

Tissue cell migration along a substrate such as the extracellular matrix (ECM) requires adhesion forces between the cell and substrate. Adhesion is necessary in order to balance propulsive forces at the leading edge of the cell that are generated by actin polymerization and contractile forces at the rear that are driven by myosin II motors [1,2]. Adhesive forces are mediated by transmembrane receptors (integrins) [3], which form one layer of a large multiprotein complex known as a focal adhesion (FA), see Fig. 1(a). More specifically, integrins are heterodimeric proteins whose extracellular domains attach to the substrate, while their intracellular domains act as binding sites for various submembrane proteins, resulting in the formation of the plaque. The plaque, which consists of more than 50 different types of protein, links the integrin layer to the actin cytoskeleton, and plays a role in intracellular signaling and force transduction.

Experimental studies of migratory cells suggests that at the leading edge, the FA acts like a molecular clutch [4–8]. That is, for high adhesion or drag, the retrograde flow of actin is slow and polymerization results in a net protrusion—the clutch is in "drive." On the other hand, if adhesion is weak, then retrograde flow can cancel the polymerization and the actin network treadmills, i.e., the clutch is in "neutral." The dynamical interplay between retrograde flow and the assembly and disassembly of focal adhesions leads to a number of behaviors that are characteristic of physical systems involving friction at moving interfaces [9–11]. These include biphasic behavior in the velocity-stress relation and stick-slip motion. The latter is a form of jerky motion, whereby a system spends most of its time in the "stuck" state and a relatively short time in the "slip" state. Various insights into the molecular clutch mechanism and its role in substrate stiffness-dependent migration have been obtained using simple stochastic models [12–17]. Such models can capture the biphasic stick-slip force velocity relation and establish the existence of an optimal substrate stiffness that is sensitive to the operating parameters of the molecular clutch.

There is growing experimental evidence that integrins or FAs also act as biochemical mechanosensors of the local microenvironment such as the rigidity and composition of the ECM [18,19]. Rigidity sensors are thought to play an important role in guiding cell migration, in particular, the ability of cells to migrate toward areas of higher ECM rigidity via a process known as *durotaxis* [20–22]. Physiological process involving durotaxis include stem cell differentiation, wound healing, development of the nervous system, and the proliferation of certain cancers (see the cited references). In order to move along a rigidity gradient, there has to be some mechanism for constantly surveying variations in the stiffness landscape of the ECM within the cellular microenvironment. Recently, high-resolution traction force microscopy has been used to characterize the nanoscale spatiotemporal dynamics of forces exerted by FAs during durotaxis [23]. These and other studies have revealed that mature FAs exhibit internal fluctuations in their traction forces, suggestive of repeated tugging on the ECM. This has led to the hypothesis that repeated FA tugging on the ECM provides a means of regularly testing the local ECM rigidity landscape over time. At least three different mechanisms for generating traction force fluctuations have been proposed [21]: Fluctuations in myosin contractility, fluctuations in the mechanics of actin stress fibers, and fluctuations in the FA molecular clutch itself. One important observation is that temporal variations are local to a single FA. That is, although neighboring FAs are mechanically coupled to each other via the actin cytoskeleton, their force fluctuations are uncorrelated [23].

The role of FAs in cell motility is related to the more general physical problem of understanding friction at moving interfaces (tribology). Some of the generic aspects of molecular bonding at sliding interfaces has been investigated in a stochastic model of single FA dynamics introduced by Sabass and Schwarz [13]. A schematic diagram of the model is shown in Fig. 1(b). The local stress fibers connected to the FA are treated as a rigid slider that moves over the substrate (retrograde flow) under the action of a constant driving force F. The latter represents the combined effects

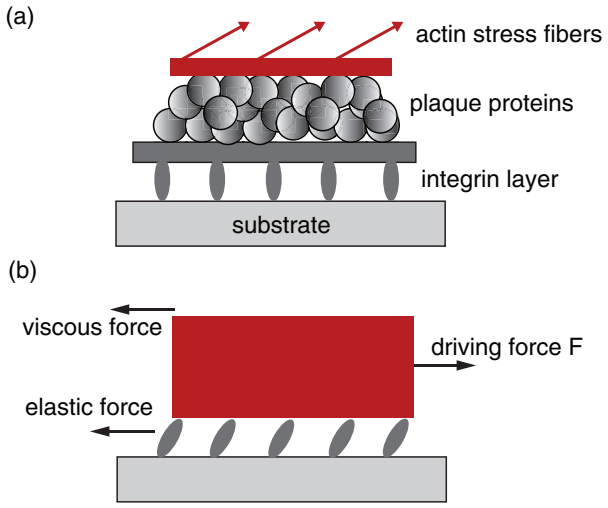

FIG. 1. (a) Schematic diagram of a FA. A layer of integrin receptors is attached to the ECM substrate and a submembrane plaque consisting of multiple proteins mediates force transmission and signaling between the integrin layer and actin stress fibers. Actin polymerization and the actomyosin contractile machinery generate forces that affect mechanosensitive proteins in the various components of the FA. (b) Simplified model of sliding friction. The driving force F for sliding is balanced by elastic adhesive forces and velocity-dependent viscous forces.

of contractile forces exerted by myosin motors at the trailing edge of the cell and actin polymerization at the leading edge. The force F is balanced by two time-dependent forces: an elastic force due to integrins that are stochastically bound at the interface and a viscous friction force ξv, where v is the sliding velocity and ξ is a friction coefficient. When a bond is attached to the cytoskeleton it stretches at the velocity v, but its extension x is immediately reset to zero whenever it unbinds. The latter occurs at an x-dependent rate $k_{\rm off}(x)$. The bond subsequently rebinds at a constant binding rate $k_{\rm on}$. The bonds are coupled due to the fact that the sliding velocity depends on the sum of the elastic forces generated by the closed bonds. However, using a mean-field approximation, one can derive an effective single-bond dynamics with a constant sliding velocity that is determined self-consistently from the single-bond statistics [13]. The mean-field model was shown to exhibit biphasic frictional behavior as a function of ξ, consistent with Monte Carlo simulations.

In this paper we extend the model from Ref. [13] by adding a stochastic component $\Delta F = \sigma \Delta W(t)$ to the driving force, where $\Delta W(t)$ is a Gaussian random variable (Wiener process) and σ is the noise strength. In terms of the application to FA adhesions dynamics, ΔF could represent fluctuations in myosin contractility or actin mechanics. The inclusion of a noise term is consistent with the Einstein relation, which implies that the noise strength and friction coefficient ξ are related according to $\sigma = \xi\sqrt{2D}$ with $D\xi = k_BT$. Here D is the diffusion coefficient of the slider, T is temperature, and k_B is the Boltzmann constant. From a mathematical perspective, the fluctuating force can be accounted for by the addition of second-order spatial derivative terms to the Chapman-Kolmogorov master equation analyzed in Ref. [13]. Indeed, this extension was briefly mentioned by the authors. However, such terms considerably complicate the analysis. In this paper we show how progress can be made by mapping the single-bond dynamics onto an equivalent single-particle system with stochastic resetting.

Stochastic resetting has generated considerable interest within the context of optimal search processes. A canonical example is a Brownian particle whose position is reset randomly in time at a constant rate r (Poissonian resetting) to some fixed point X_r, which could be its initial position. This system exhibits two of the major features observed in more complex models: (i) convergence to a nontrivial nonequilibrium stationary state (NESS) and (ii) the mean time for a Brownian particle to find a hidden target is finite and has an optimal value as a function of the resetting rate r [24–26]. There have been numerous studies of more general stochastic processes with both Poissonian and non-Poissonian resetting, memory effects, and spatially extended systems, see the recent review [27] and references therein. In the particular case of bond dynamics, the extension of a bond represents the position of a particle that resets to the origin at a spatially dependent resetting rate $r(x) = k_{\rm off}(x)$, after which it remains at the origin for a refractory period of mean duration $k_{\rm on}^{-1}$. If Brownian motion of the sliding cytoskeleton is included, then the system behaves as an overdamped Brownian particle moving in a potential well [28] and subject to spatially dependent resetting [29] and a refractory period [30]. The advantage of formulating bond dynamics in terms of a process with stochastic resetting is that one can apply various analytical tools, including renewal theory and path integral methods.

The structure of the paper is as follows. The basic sliding friction model is introduced in Sec. II, which takes the form of a stochastic hybrid system that couples the continuous dynamics of bond stretching with the Markov chain for binding and unbinding. We also construct the differential Chapman-Kolmogorov (CK) equation for the evolution of the corresponding joint probability density. In Sec. III we consider the case of a single bond and show how the resulting system can be reinterpreted in terms of an overdamped Brownian particle with spatially dependent stochastic resetting. We derive a general expression for the steady-state density of the single-particle CK equation by extending the renewal theory of Ref. [29]. We then calculate the density in the case of constant sliding velocity v_0 and a parabolic resetting function. In Sec. IV, we show how the multibond system can be reduced to the single-particle model of Sec. III using a mean-field approximation along analogous lines to Ref. [13]. This yields an equation relating v_0 to the mean traction force. We thus show how diffusion can sharpen the response to changes in the effective stiffness of the adhesion bonds. This is consistent with the hypothesis that force fluctuations could play a role in mechanosensing of the local microenvironment.

II. STOCHASTIC MODEL OF SLIDING FRICTION

We begin by describing the model of sliding friction considered in Ref. [13] and illustrated in Fig. 1(b). Suppose that the FA is of constant size so that there is a fixed maximal number of N assembled bonds. Each bond, $i = 1, \ldots, N$, can be in one of two states denoted by $q_i(t) \in \{0, 1\}$, with the bond closed (open) if $q_i(t) = 1$ [$q_i(t) = 0$]. The closed bonds

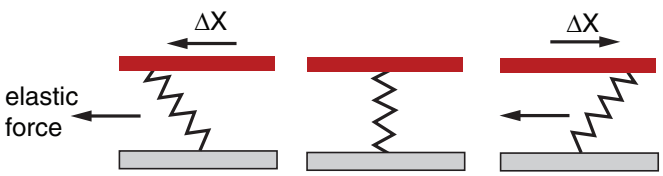

FIG. 2. Illustration of how both positive and negative displacements of a closed bond result in an extension of the equivalent Hookean spring and an elastic force that opposes the driving force.

are modeled as Hookean springs with spring constant κ and time-dependent extension that stretches at the sliding velocity v. On the other hand, an open bond is assumed to immediately reset to its equilibrium state of zero extension. Let $x_i(t)$ denote the extension of the ith bond attachment point at time t relative to its equilibrium value. Whenever the bond is attached, its displacement from equilibrium is given by $dx_i(t) = dX(t)$, where $X(t)$ is the current position of the slider. The velocity v of the latter is determined by a force-balance equation, which takes the form [13]

$$v = v(\mathbf{x}) := \frac{1}{\xi}\left[F - \kappa \sum_{i=1}^{N} q_i(t)x_i(t)\right], \tag{2.1}$$

with $\mathbf{x} = (x_1, \ldots, x_N)^\top$. Here F is the constant driving force and ξ is a friction coefficient. The displacements x_i thus evolve according to the system of equations

$$\frac{dx_i}{dt} = v(\mathbf{x}) \text{ if } q_i(t) = 1, \quad x_i = 0 \text{ if } q_i(t) = 0, \tag{2.2}$$

with $i = 1, \ldots, N$ and $v(\mathbf{x}) \geqslant 0$. Finally, the stochastic switching of the discrete state $q_i(t)$ between the values 0,1 is determined by a constant binding rate $k_{\rm on}$ and a stretch-dependent off-rate given by the Bell-Evans formula [2,31,32]

$$r(x) = k_{\rm off} e^{\kappa x/F_b}, \tag{2.3}$$

where F_b is the characteristic bond rupture force.

The stochasticity of the model introduced in Ref. [13] arises from the assembly and disassembly of the bonds according to the switching rates $k_{\rm on}$ and $r(x_i)$. In this paper we wish to incorporate another source of noise, namely fluctuations in the force F. The latter appears as a single additive term in the force-balance equation (2.1) such that $F \to F + \Delta F$. The piecewise deterministic system (2.2) is now replaced by the SDE

$$dX_i(t) = v(\mathbf{X})dt + \sqrt{2D}dW(t) \quad \text{for } q_i(t) = 1, \tag{2.4}$$

where $\Delta F/\xi = \sqrt{2D}dW(t)$ and $W(t)$ is a Wiener process:

$$\langle dW(t)\rangle = 0, \quad \langle dW(t)dW(t')\rangle = \delta(t - t')dt\, dt'. \tag{2.5}$$

This is supplemented by the reset condition $X_i(t) = 0$ for $q_i(t) = 0$. It can be seen that all bonds are subject to a common stochastic drive. One major difference from the $D = 0$ case is that it is possible for a closed bond to be subject to negative displacements. That is, if we reinterpret $X_i(t)$ as the (stochastic) position of the ith bond attachment point at time t relative to its equilibrium value, then although $v(\mathbf{X}) \geqslant 0$, the presence of Gaussian noise allows $X_i(t) < 0$. As it stands, this would represent a compression of the corresponding spring, resulting in a force component that is in the same direction as F. Suppose that compressive forces cannot occur. One way to deal with this would be to add a reflecting boundary condition for each bond at $X_i = 0$ along the lines of Ref. [13]. However, this considerably complicates the analysis in the presence of diffusion. A second option is illustrated in Fig. 2, which shows how negative displacements could also result in an extension of the Hookean spring so that the corresponding elastic force still opposes the driving force. This requires modifying the original model by taking

$$v(\mathbf{x}) := \frac{1}{\xi}\left[F - \kappa \sum_{i=1}^{N} q_i(t)|x_i(t)|\right], \tag{2.6}$$

and

$$r(x) = k_{\rm off} e^{\kappa|x|/F_b}. \tag{2.7}$$

(Figure 2 also suggests that there should be some geometrical factor that converts horizontal displacements of the slider to extensions of the spring. To take proper account of the geometry one would need to consider a more detailed model of the mechanical properties of the system beyond the level considered here. Therefore, as in Ref. [13], we ignore this complication.) In this paper we will take $x_i \in \mathbb{R}$ and $v(\mathbf{x})$ to be given by Eq. (2.6). However, if D is sufficiently small then the probability of negative displacements is also small so that similar results would be obtained using Eq. (2.1) for $v(\mathbf{x})$. (An analogous approximation is often carried out in system-size expansions of chemical master equations in which molecular concentrations are positive [33].)

The above dynamical system is an example of a stochastic hybrid system, since it couples a set of continuous variable $\mathbf{x}(t)$ with a Markov chain for the discrete states $\mathbf{q} = (q_1, \ldots, q_N)$. Let $\rho(\mathbf{x}, t, \mathbf{q})$ denote the probability density that at time t the bonds are in the configurational state $\mathbf{q}$ and have displacements $\mathbf{x}$. (Note that $x_j = 0$ for all j such that $q_j = 0$.) As shown in Ref. [13] for $D = 0$, $\rho(\mathbf{x}, t, \mathbf{q})$ evolves according to a differential CK equation. In between the closing or opening of any bonds, the displacements of all the closed bonds evolve according to a multivariate Fokker-Planck equation. Whenever the ith bond opens, its displacement x_i is immediately reset to zero and, after an exponentially distributed waiting time with rate $k_{\rm on}$, it reattaches and the bond starts stretching again. These switching processes generate reaction terms in the CK equation. The latter takes the form

$$\frac{\partial \rho(\mathbf{x}, t, \mathbf{q})}{\partial t} = -\sum_{i=1}^{N} q_i \frac{\partial J(\mathbf{x}, t, \mathbf{q})}{\partial x_i} - \sum_{i=1}^{N} q_i r(x_i)\rho(\mathbf{x}, t, \mathbf{q}) - \sum_{i=1}^{N}(1 - q_i)k_{\rm on}\rho(\mathbf{x}, t, \mathbf{q})$$
$$+ \sum_{i=1}^{N} \delta(x_i)\left\{(1 - q_i)\int_{-\infty}^{\infty} r(x_i')\,\rho(\mathbf{x}, t, \mathbf{q})|_{(x_i, q_i)=(x_i', 1)}dx_i' + q_i k_{\rm on}\rho(\mathbf{x}, t, \mathbf{q})|_{q_i=0}\right\}, \tag{2.8}$$

where

$$J(\mathbf{x},t,\mathbf{q}) = -D\sum_{j=1}^{N} q_j \frac{\partial \rho(\mathbf{x},t,\mathbf{q})}{\partial x_j} + v(\mathbf{x})\rho(\mathbf{x},t,\mathbf{q}). \quad (2.9)$$

The first summation on the right-hand side of Eq. (2.8) represent the advection-diffusion of closed bonds in between switching events. Note that the diffusion matrix is $D_{ij} = D$ for all i, j rather than the standard diagonal matrix $D_{ij} = D\delta_{i,j}$, which is due to the fact that all bonds are driven by a common Brownian motion. The next two summations represent reaction terms associated with the unbinding and binding of bonds. Finally, the terms in the bracket $\{\cdot\}$ represent the fluxes into the state $x_i = 0$ due to unbinding of the ith bond in the closed state followed by resetting, and binding of the ith bond in the open state. Total probability is then conserved, as can be shown by integrating both sides of Eq. (2.8) with respect to $\mathbf{x}$ and summing over all configurations $\mathbf{q}$:

$$\frac{d}{dt}\left\{\sum_{\mathbf{q}}\left[\prod_{j=1}^{N}\int_{-\infty}^{\infty} dx_j\right]\rho(\mathbf{x},t,\mathbf{q})\right\} = 0. \quad (2.10)$$

Equation (2.8) reduces to the CK equation of Ref. [13] when $D = 0$ [34]. The latter authors calculated the resulting steady-state probability density using a mean-field approximation. This involved taking the large-N limit and replacing $v(\mathbf{x})$ by a space-independent mean velocity v_0. The resulting probability density then factorizes into the product of N single-bond densities, which can be used to derive a self-consistency condition for v_0. Extending such an analysis to take into account the effects of diffusion is nontrivial. In this paper we show how progress can be made by mapping the given system on to a dynamical process with stochastic resetting [27]. Making the connection between FA bond dynamics and stochastic resetting means that we can combine the mean-field approach of Ref. [13] with recent results concerning single-particle dynamics with stochastic resetting [29]. Therefore, the first step is to consider the case of a single bond ($N = 1$).

One final remark is in order. Since the drift velocity is taken to be a constant v_0 under the mean-field approximation, the resulting solution of the CK equation is independent of whether we take the force-balance equation to be (2.1) or (2.6), for example. The latter only plays a role in determining the relationship between traction forces and the velocity v_0, see Sec. IV. However, the corresponding choice of resetting rate $r(x)$ does affect the probability density. In particular, we will show how an explicit solution for the density can be obtained when $r(x)$ is an even, parabolic function of x. (Mathematically speaking, the analysis reduces to calculating the quantum propagator for a particle in a harmonic potential, see Sec. III C.) This is consistent with the assumption that both negative and positive displacements stretch a bond. Note, however, that for slow diffusion the displacements will be predominantly positive so that taking $r(x)$ to be an even function is not a strong constraint.

III. ANALYSIS OF A SINGLE BOND ($N = 1$)

Setting $x_1 = x$, $\rho(x,t,1) = p(x,t)$ and $\rho(0,t,0) = P_0(t)$, Eq. (2.8) reduces to the pair of equations

$$\frac{\partial p(x,t)}{\partial t} = D\frac{\partial^2 p(x,t)}{\partial x^2} - \frac{\partial v(x)p(x,t)}{\partial x} - r(x)p(x,t) + \delta(x)k_{\rm on}P_0(t), \quad (3.1a)$$

$$\frac{dP_0(t)}{dt} = -k_{\rm on}P_0(t) + \int_{-\infty}^{\infty} r(x')p(x',t)dx'. \quad (3.1b)$$

Here $J(x,t)$ is the probability flux

$$J(x,t) = -D\frac{\partial p}{\partial x} + v(x)p(x,t), \quad (3.2)$$

with $v(x)$ determined by the force balance equation. [Later we will set $v(x) = v_0$.] The distributions satisfy the normalization condition

$$\int_{-\infty}^{\infty} p(x,t)dx + P_0(t) = 1. \quad (3.3)$$

In the fast binding limit, $k_{\rm on} \to \infty$, Eq. (3.1) reduces to the scalar equation

$$\frac{\partial p(x,t)}{\partial t} = D\frac{\partial^2 p(x,t)}{\partial x^2} - \frac{\partial v(x)p(x,t)}{\partial x} - r(x)p(x,t) + \delta(x)\int_{-\infty}^{\infty} r(x')p(x',t)dx'. \quad (3.4)$$

A crucial observation is that Eq. (3.1) is identical in form to the CK equation for an overdamped Brownian particle moving in a potential landscape $V(x)$, where $v(x) = -V'(x)/\xi$, and subject both to spatially dependent resetting and a refractory period. That is, we can identify $r(x)$ as a spatially dependent resetting rate [29], $x = 0$ as the resetting position, and $k_{\rm on}^{-1}$ as the mean time spent in a refractory state following resetting [30]. Thus $P_0(t)$ is the probability of being in the refractory state at time t. In the absence of a refractory period, this type of process has recently been analyzed using a path-integral formalism [29], see also Ref. [28]. We will extend this approach in order to include a refractory period. Since the analysis applies more generally than to the particular model of bond dynamics, we consider general positive functions $r(x)$, $v(x)$ and assume that the particle spends a refractory period σ following each return to the origin, with σ generated from a waiting time density $\psi(\sigma)$. In the case of bond dynamics,

$$\psi(\sigma) = k_{\rm on}e^{-k_{\rm on}\sigma}. \quad (3.5)$$

A. Renewal equation

A typical method for analyzing the CK equation of a process with stochastic resetting is to use renewal theory [27]. Here we follow the particular formulation of Ref. [29], which we extend to take into account the refractory period. Let $\Pi(x,t)$ denote the probability density that the particle starts at the origin and ends at x at time t without undergoing any reset

event. We can then write down the (last) renewal equation

$$p(x,t) = \Pi(x,t) + \int_0^t d\tau \left[\int_0^{t-\tau} d\sigma\, \psi(\sigma) R(t-\tau-\sigma)\right] \Pi(x,\tau), \tag{3.6}$$

where

$$R(t) = \int_{-\infty}^{\infty} r(y) p(y,t) dy \tag{3.7}$$

is the probability density of resetting at time t. The first term on the right-hand side represents all trajectories that reach x without resetting, while the second term sums over trajectories that last reset at time $t-\tau-\sigma$, spent a time σ in the refractory state, exited the refractory state at time $t-\tau$, and then propagated from the origin to x without any further reset events.

Introduce the probability density that the first reset is at time t,

$$F(t) = \int_{-\infty}^{\infty} r(y) \Pi(y,t) dy, \tag{3.8}$$

with $\int_0^\infty F(t)dt = 1$. Multiplying both sides of Eq. (3.6) by $r(x)$ and integrating with respect to x gives

$$\begin{aligned} R(t) &= \int_{-\infty}^{\infty} r(x)\Pi(x,t)dx + \int_0^t d\tau \int_{-\infty}^{\infty} dx\, r(x)\Pi(x,\tau) \\ &\quad \times \left[\int_0^{t-\tau} d\sigma\, \psi(\sigma) R(t-\tau-\sigma)\right] \\ &= F(t) + \int_0^t d\tau F(\tau)\left[\int_0^{t-\tau} d\sigma\, \psi(\sigma) R(t-\tau-\sigma)\right]. \end{aligned} \tag{3.9}$$

Laplace transforming this equation shows that

$$\widetilde{R}(s) = \widetilde{F}(s) + \widetilde{F}(s)\widetilde{\psi}(s)\widetilde{R}(s),$$

which can be rearranged to give

$$\widetilde{R}(s) = \frac{\widetilde{F}(s)}{1-\widetilde{\psi}(s)\widetilde{F}(s)}. \tag{3.10}$$

Laplace transforming the renewal integral equation (3.6) and using Eq. (3.10), we then have

$$\widetilde{p}(x,s) = \widetilde{\Pi}(x,s)[1+\widetilde{\psi}(s)\widetilde{R}(s)] = \frac{\widetilde{\Pi}(x,s)}{1-\widetilde{\psi}(s)\widetilde{F}(s)}.$$

Hence, the Laplace transform of the probability density with resetting can be determined completely from the Laplace transforms of the probability density without resetting and the waiting time density:

$$\widetilde{p}(x,s) = \frac{\widetilde{\Pi}(x,s)}{1-\widetilde{\psi}(s)\int_{-\infty}^{\infty} r(y)\widetilde{\Pi}(y,s)dy}. \tag{3.11}$$

This recovers the result of Ref. [29] when $\widetilde{\psi}(s) = 1$. Finally, given the Laplace transform, we can obtain the steady-state density using the final value theorem:

$$\begin{aligned} p^*(x) &= \lim_{t\to\infty} p(x,t) = \lim_{s\to 0} s\widetilde{p}(x,s) \\ &= \lim_{s\to 0} \frac{s\widetilde{\Pi}(x,s)}{1-\widetilde{\psi}(s)\widetilde{F}(s)}. \end{aligned} \tag{3.12}$$

Since $\widetilde{\psi}(0) = 1 = \widetilde{F}(0)$, we need to evaluate the limit using L'Hopital's rule, which yields:

$$p^*(x) = -\frac{\widetilde{\Pi}(x,0)}{\widetilde{\psi}'(0)+\widetilde{F}'(0)} = \frac{\widetilde{\Pi}(x,0)}{\overline{\sigma}+T_{\rm res}}, \tag{3.13}$$

where

$$\overline{\sigma} = \int_0^\infty \sigma\psi(\sigma)d\sigma, \quad T_{\rm res} = \int_0^\infty tF(t)dt. \tag{3.14}$$

Here $\overline{\sigma}$ is the mean refractory period and $T_{\rm res}$ is the mean first-reset time. It is important to note that the density $p^*(x)$ is an example of a NESS, since the steady-state fluxes at $x=0$ are nonzero due to resetting. This is a characteristic feature of dynamical systems with stochastic resetting.

A useful check of the above calculation is to make sure that it is consistent with conservation of total probability. Integrating Eq. (3.11) with respect to x gives

$$\int_{-\infty}^{\infty} \widetilde{p}(x,s)dx = \frac{\int_{-\infty}^{\infty}\widetilde{\Pi}(x,s)dx}{1-\widetilde{\psi}(s)\widetilde{F}(s)}. \tag{3.15}$$

In the absence of a refractory period, $\widetilde{\psi}(s) = 1$ and the normalization condition is

$$\int_{-\infty}^{\infty} p(x,t)dx = 1.$$

Hence

$$\int_0^\infty \widetilde{\Pi}(x,s)dx = \frac{1-\widetilde{F}(s)}{s}.$$

Since the trajectories contributing to $\Pi(x,t)$ do not involve any resetting events, this equation also holds when there is a refractory period. Substituting into Eq. (3.15) thus yields

$$\begin{aligned} \int_{-\infty}^{\infty}\widetilde{p}(x,s)dx &= \frac{1-\widetilde{F}(s)}{s[1-\widetilde{\psi}(s)\widetilde{F}(s)]} \\ &= \frac{1}{s} - \frac{1-\widetilde{\psi}(s)}{s}\frac{\widetilde{F}(s)}{[1-\widetilde{\psi}(s)\widetilde{F}(s)]} \\ &= \frac{1}{s} - \frac{1-\widetilde{\psi}(s)}{s}\widetilde{R}(s) = \frac{1}{s} - \frac{\widetilde{R}(s)}{s+k_{\rm on}}. \end{aligned}$$

We have used the explicit form for $\psi(\sigma)$. Finally, Laplace transforming Eq. (3.1 b) gives

$$\widetilde{P}_0(s) = \frac{\widetilde{R}(s)}{s+k_{\rm on}},$$

so that

$$\int_{-\infty}^{\infty}\widetilde{p}(x,s)dx + \widetilde{P}_0(s) = \frac{1}{s},$$

which is the Laplace transform of the probability conservation condition (3.3).

B. Calculation of $\Pi(x,t)$ for constant r

The above application of renewal theory has shown that the steady-state probability density $p^*(x)$ of a Brownian particle with spatially dependent resetting and refractory periods can be expressed in terms of the Laplace transform of the probability density without any resetting, $\Pi(x,t)$. Unfortunately, obtaining explicit expression for $\widetilde{\Pi}(x,s)$ is not possible except for particular choices of $v(x)$ and $r(x)$ [28,29].

In the case of a constant resetting rate $r(x)=r_0$, $\Pi(x,t)$ is simply the product of the probability $e^{-r_0 t}$ of no resetting over a time interval t and the Neumann Green's function of the Fokker-Planck equation without resetting [27]. That is,

$$\Pi(x,t)=e^{-r_0 t}G(x,t|0,0), \tag{3.16}$$

where

$$\frac{\partial G}{\partial t}=D\frac{\partial^2 G}{\partial x^2}-\frac{\partial v(x)G}{\partial x}, \tag{3.17}$$

$G(x,0|x_0,0)=\delta(x-x_0)$, and

$$v(0)G(0,t|x_0,0)-D\left.\frac{\partial G(x,t|x_0,0)}{\partial x}\right|_{x=0}=0. \tag{3.18}$$

The Laplace transform of $\Pi(x,t)$ is thus

$$\begin{aligned}\widetilde{\Pi}(x,s)&=\int_{-\infty}^{\infty}e^{-(s+r_0)t}G(x,t|0,0)dt\\&=\widetilde{G}(x,s+r_0|0,0).\end{aligned} \tag{3.19}$$

Since $\int_{-\infty}^{\infty}G(x,t|0,0)dx=1$, we have

$$\int_{-\infty}^{\infty}\widetilde{\Pi}(x,s)dx=\frac{1}{r_0+s}.$$

Substituting into Eq. (3.11) then yields the steady-state density

$$\begin{aligned}p^*(x)&=\lim_{s\to 0}\frac{s\widetilde{G}(x,s+r_0|0,0)}{1-r_0\widetilde{\psi}(s)\int_0^{\infty}\widetilde{G}(y,s+r_0|0,0)dy}\\&=\widetilde{G}(x,r_0|0,0)\left[-r_0\frac{d}{ds}\frac{\widetilde{\psi}(s)}{s+r_0}\right|_{s=0}\Bigg]^{-1}\\&=\frac{\widetilde{G}(x,r_0|0,0)}{\overline{\sigma}+r_0^{-1}}.\end{aligned} \tag{3.20}$$

We have used L'Hopital's rule and

$$\widetilde{\psi}(0)=1,\quad -\widetilde{\psi}'(0)=\overline{\sigma}:=\int_0^{\infty}\sigma\psi(\sigma)d\sigma. \tag{3.21}$$

A further simplification is to take $v(x)=v_0$. This will turn out to be the relevant form of the effective drift velocity under the mean-field approximation for large N, see Sec. IV. In the case of constant drift, we have

$$G(x,t|0,0)=\frac{1}{\sqrt{4\pi Dt}}e^{-(x-v_0t)^2/4Dt}. \tag{3.22}$$

Performing the Laplace transform and substituting into Eq. (3.20) yields

$$p^*(x)=\frac{1}{\overline{\sigma}+r_0^{-1}}\frac{1}{\sqrt{4Dr_0+v_0^2}}e^{xv_0/2D}e^{-\sqrt{4Dr_0+v_0^2}x/D}. \tag{3.23}$$

C. Calculation of $\Pi(x,t)$ for spatially dependent resetting

The calculation of $\Pi(x,t)$ for spatially dependent resetting is considerably more involved. One approach is to use an eigenfunction expansion of the propagator as briefly summarized in the Appendix. Here we follow the analysis of Ref. [29], which establishes that the probability density $\Pi(x,t)$ can be expressed in terms of a path integral on $\mathbb{R}$ of the form

$$\Pi(x,t)=\int_{x(0)=0}^{x(t)=x}e^{-S[x]}\mathcal{D}[x],\quad x>0, \tag{3.24}$$

where $\mathcal{D}[x]$ is the appropriate Wiener measure and $S[x]$ is the action

$$S[x]=\int_0^t\left\{\frac{[\dot{x}-v(x)]^2}{4D}+\frac{v'(x)}{2}+r(x)\right\}dt. \tag{3.25}$$

For particular choices of $v(x)$ and $r(x)$, the path integral can be evaluated by formally identifying it with the propagator $\mathcal{G}$ of a quantum mechanical system on $\mathbb{R}$ that evolves in imaginary time [29]:

$$\Pi(x,t)=\exp\left[\frac{1}{2D}\int_0^x v(y)dy\right]\mathcal{G}(x,-it|0,0), \tag{3.26}$$

where

$$\mathcal{G}(x,-it|x_0,0)=\langle x|e^{-\widehat{H}t}|x_0\rangle. \tag{3.27}$$

Here $\widehat{H}$ is the Hamiltonian operator

$$\widehat{H}=-D\frac{\partial^2}{\partial x^2}+U(x) \tag{3.28}$$

of a quantum particle of mass $m=1/2D$ (assuming Planck's constant $\hbar=1$) subject to the potential

$$U(x)=\frac{v(x)^2}{4D}+\frac{v'(x)}{2}+r(x). \tag{3.29}$$

We will restrict the analysis to a constant drift, $v(x)=v_0$, and set $r(x)=r_0+\Delta r(x)$ with $\Delta(0)=0$. Then

$$\Pi(x,t)=e^{-(v_0^2/4D+r_0)t}e^{xv_0/2D}\mathcal{G}_r(x,-it|0,0), \tag{3.30}$$

where $\mathcal{G}_r$ is the quantum propagator for the Hamiltonian

$$\widehat{H}=-D\frac{\partial^2}{\partial x^2}+\Delta r(x). \tag{3.31}$$

Even for this case, there are only very few choices of $\Delta r(x)$ for which an exact expression for the quantum propagator is known [35,36]. Although these do not include an exponential resetting rate, $r(x)=r_0e^{\kappa x/F_b}$, one can determine the propagator for a parabolic resetting rate

$$r(x)=k_{\rm off}(1+3\kappa^2x^2/F_b^2), \tag{3.32}$$

see Ref. [29]:

$$\begin{aligned}\mathcal{G}_r(x,-it|0,0)&=\frac{(\alpha/D)^{1/4}}{\sqrt{2\pi\sinh(t\sqrt{4D\alpha})}}\\&\times\exp\left[-\frac{x^2\sqrt{\alpha/D}}{2\tanh(t\sqrt{4D\alpha})}\right],\end{aligned} \tag{3.33}$$

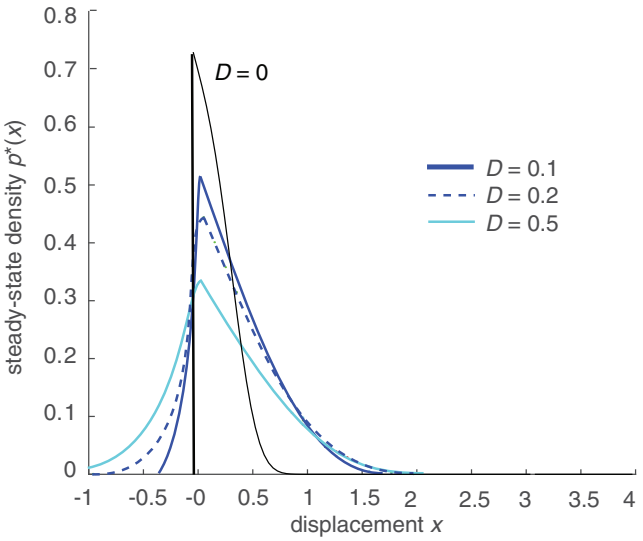

FIG. 3. Plot of steady-state density $p^*(x)$ for different diffusivities D and $v_0 = \kappa = 1$. Other parameters are at baseline values.

where $\alpha = 3r_0\kappa^2/F_b^2$. The steady-state density $p^*(x)$ for a given drift v_0 is then given by Eq. (3.13) with $\overline{\sigma} = k_{\rm on}^{-1}$:

$$\widetilde{\Pi}(x,0) = e^{xv_0/2D}\int_0^\infty e^{-(v_0^2/4D+r_0)t}\frac{(\alpha/D)^{1/4}}{\sqrt{2\pi\,\sinh(t\sqrt{4D\alpha})}} \times \exp\left[-\frac{x^2\sqrt{\alpha/D}}{2\tanh(t\sqrt{4D\alpha})}\right]dt, \tag{3.34}$$

and

$$T_{\rm res} = \int_0^\infty te^{-(v_0^2/4D+r_0)t}\frac{(\alpha/D)^{1/4}}{\sqrt{2\pi\,\sinh(t\sqrt{4D\alpha})}} \times \left\{\int_0^\infty r(x)e^{xv_0/2D}\exp\left[-\frac{x^2\sqrt{\alpha/D}}{2\tanh(t\sqrt{4D\alpha})}\right]dx\right\}dt. \tag{3.35}$$

These integrals are evaluated numerically. In Fig. 3 we show sample plots of $p^*(x)$ for fixed $v_0 = 1$ and various diffusivities D. Note that $p^*(x)$ is strongly skewed towards positive values of x for small D, that is, for $D \ll v_0$ in dimensionless units.

D. Zero diffusion limit

A useful check of the above analysis is to take the limit $D \to 0$ and compare the resulting asymptotic behavior of $p^*(x)$ with the solution obtained by setting $D = 0$ in the steady-state version of Eq. (3.1). The latter takes the form

$$0 = D\frac{d^2p^*(x)}{dx^2} - v_0\frac{dp^*(x)}{dx} - r(x)p^*(x) + \delta(x)k_{\rm on}P_0^*, \tag{3.36}$$

together with the normalization condition

$$\int_0^\infty p^*(x)dx + P_0^* = 1. \tag{3.37}$$

In the case $D = 0$, we have $x \geqslant 0$ and Eq. (3.36) becomes

$$v_0\frac{dp^*}{dx} = -r(x)p^*(x), \tag{3.38}$$

with the boundary condition $p^*(0) = k_{\rm on}P_0^*/v_0$. The solution is

$$p^*(x) = \frac{P_0^*k_{\rm on}}{v_0}\exp\left[-\frac{1}{v_0}\int_0^x r(y)dy\right] = \frac{P_0^*k_{\rm on}}{v_0}\exp\left[-\frac{k_{\rm off}}{v_0}(x+\kappa^2x^3)\right]. \tag{3.39}$$

The constant P_0^* is then determined using the normalization condition,

$$P_0^*\left\{1 + \frac{k_{\rm on}}{v_0}\int_0^\infty \exp\left[-\frac{1}{v_0}\int_0^x r(y)dy\right]dx\right\} = 1. \tag{3.40}$$

Substituting for $r(x)$ using Eq. (3.32), we have

$$P_0^*\left\{1 + \frac{k_{\rm on}}{v_0}\int_0^\infty \exp\left[-\frac{k_{\rm off}}{v_0}(x+\kappa^2x^3)\right]dx\right\},$$

which can be arranged to give

$$P_0^* = \left\{1 + \frac{\gamma k_{\rm on}}{k_{\rm off}}\int_0^\infty \exp\left([-\gamma(y+y^3)]\right)dy\right\}^{-1},$$

with $\gamma = k_{\rm off}/(v_0\kappa)$.

The integral term in the expression for P_0^* can be expressed as an infinite sum over gamma functions. That is,

$$I_0(\gamma) := \int_0^\infty \exp[-\gamma(y+y^3)]dy = \sum_{n=0}^\infty \frac{(-\gamma)^n}{n!}\int_0^\infty y^n e^{-\gamma y^3}dy = \sum_{n=0}^\infty \frac{(-\gamma)^n}{n!}\int_0^\infty \left(\frac{t}{\gamma}\right)^{n/3}e^{-t}\frac{dt}{3(\gamma t^2)^{1/3}}.$$

We have Taylor expanded $e^{-\gamma y}$, rearranged the order of summation and integration, and performed the change of integration variables $t = \gamma y^3$. Recalling the definition of the gamma function,

$$\Gamma(z) = \int_0^\infty t^{z-1}e^{-t}, \tag{3.41}$$

$I_0(\gamma)$ can be rewritten as

$$I_0(\gamma) = \sum_{n=0}^\infty \frac{(-1)^n}{3n!}\gamma^{(2n-1)/3}\Gamma\left(\frac{n+1}{3}\right), \tag{3.42}$$

such that

$$P_0 = P_0^*(\gamma) := \left[1 + \frac{\gamma k_{\rm on}}{k_{\rm off}}I_0(\gamma)\right]^{-1}. \tag{3.43}$$

In the small diffusion limit, we can carry out an asymptotic expansion of the integral in Eq. (3.34). That is, the factor $e^{-v_0^2/4Dt}$ implies that the integral is dominated by contributions close to $t = 0$ so that we can Taylor expand the sinh and tanh functions:

$$\begin{aligned}
\widetilde{\Pi}(x,0) &\approx e^{xv_0/2D}\int_0^\infty e^{-(v_0^2/4D+k_{\rm off})t}\frac{(\alpha/D)^{1/4}}{\sqrt{2\pi\, t\sqrt{4D\alpha}}}\exp\left\{-\frac{x^2\sqrt{\alpha/D}}{2[t\sqrt{4D\alpha}-(t\sqrt{4D\alpha})^3/3]}\right\}dt\\
&\approx e^{xv_0/2D}\int_0^\infty e^{-(v_0^2/4D+k_{\rm off})t}\frac{1}{\sqrt{4\pi Dt}}\exp\left\{-\frac{x^2}{4Dt[1-4D\alpha t^2/3]}\right\}dt\\
&\approx e^{xv_0/2D}\int_0^\infty e^{-(v_0^2/4D+k_{\rm off}+\alpha x^2/3)t}\frac{1}{\sqrt{4\pi Dt}}\exp\left(-\frac{x^2}{4Dt}\right)dt\\
&= e^{xv_0/2D}\int_{-\infty}^\infty e^{ikx}\left\{\int_0^\infty e^{-(v_0^2/4D+k_{\rm off}+\alpha x^2/3)t}e^{-Dk^2t}dt\right\}\frac{dk}{2\pi}\\
&= e^{xv_0/2D}\int_{-\infty}^\infty \frac{e^{ikx}}{Dk^2+v_0^2/4D+k_{\rm off}+\alpha x^2/3}\frac{dk}{2\pi}\\
&= \frac{1}{\sqrt{v_0^2+4D(k_{\rm off}+\alpha x^3/3)}}\exp\left[\frac{v_0x}{2D}-\frac{v_0|x|}{2D}\sqrt{1+\frac{4D(k_{\rm off}+\alpha x^2/3)}{v_0^2}}\right].
\end{aligned}$$

We have used contour integration to evaluate the final k integral. Finally, Taylor expanding the square-root functions to leading order shows that

$$\widetilde{\Pi}(x,0)\sim\frac{1}{v_0}e^{-x(k_{\rm off}+\alpha x^2/3)/v_0}$$

for $x>0$ and

$$\widetilde{\Pi}(x,0)\sim\frac{1}{v_0}e^{-|x|v_0/D}$$

for $x<0$. Hence, if $x>0$, then we recover the x dependence of $p^*(x)$ given by Eq. (3.39) for $D=0$. On the other hand, if $x<0$, then $p^*(x)\to 0$ as $D\to 0$. These results are consistent with Fig. 3.

IV. MULTIPLE ADHESION BONDS AND MEAN-FIELD THEORY

We now extend the mean-field approach of Ref. [13] in order to reduce the CK equation (2.8) to an effective single-particle CK equation with constant drift v_0. The force-balance equation is then used to derive a self-consistency condition relating the mean traction force and v_0.

A. Mean-field approximation (fast binding limit)

It is convenient to first consider the fast binding limit $k_{\rm on}\to\infty$. Equation (2.8) for $\rho(\mathbf{x},t)=\rho(\mathbf{x},t,\mathbf{q})|_{\mathbf{q}=(1,\ldots,1)}$ can then be written in the more compact form

$$\begin{aligned}
\frac{\partial\rho(\mathbf{x},t)}{\partial t} &= -\sum_{i=1}^N\frac{\partial J(\mathbf{x},t)}{\partial x_i}-\sum_{i=1}^N r(x_i)\rho(\mathbf{x},t),\\
&\quad+\sum_{i=1}^N\delta(x_i)\int_{-\infty}^\infty r(x_i')\,\rho(\mathbf{x},t)|_{x_i=x_i'}dx_i'. \qquad (4.1)
\end{aligned}$$

The probability flux is

$$J(\mathbf{x},t)=-D\sum_{j=1}^N\frac{\partial\rho(\mathbf{x},t)}{\partial x_i}+v(\mathbf{x})\rho(\mathbf{x},t). \qquad (4.2)$$

Consider a particular bond labeled k and integrate both sides of Eq. (4.1) with respect to x_j for all $j\neq k$. Defining

$$\rho_k(x,t)=\left[\prod_{j=1}^N\int_{-\infty}^\infty dx_j\right]\delta(x_k-x)\rho(\mathbf{x},t), \qquad (4.3)$$

and

$$J_k(x,t)=\left[\prod_{j=1}^N\int_{-\infty}^\infty dx_j\right]\delta(x_k-x)J(\mathbf{x},t), \qquad (4.4)$$

we find that

$$\begin{aligned}
\frac{\partial\rho_k(x,t)}{\partial t} &= -\frac{\partial J_k(x,t)}{\partial x_k}-r(x)\rho_k(x,t)\\
&\quad+\delta(x_k)\int_{-\infty}^\infty r(x')\rho_k(x',t)dx'. \qquad (4.5)
\end{aligned}$$

Unfortunately, Eq. (4.5) is not a closed single-particle CK equation, since $J_k(x,t)$ depends on the full probability density $\rho(\mathbf{x},t)$. That is, substituting Eq. (4.2) into (4.4) gives

$$\begin{aligned}
J_k(x,t) &= \left[\prod_{j=1}^N\int_{-\infty}^\infty dx_j\right]\delta(x_k-x)\\
&\quad\times\left[-D\frac{\partial\rho(\mathbf{x},t)}{\partial x_k}+v(\mathbf{x})\rho(\mathbf{x},t)\right]\\
&= -D\frac{\partial\rho_k(x,t)}{\partial x}\\
&\quad+\left[\prod_{j=1}^N\int_{-\infty}^\infty dx_j\right]\delta(x_k-x)v(\mathbf{x})\rho(\mathbf{x},t). \qquad (4.6)
\end{aligned}$$

The mean-field approximation is to assume that for large N, the individual bonds are statistically independent so that we can factorize the multibond density into the product of N

single-bond densities:

$$\rho(\mathbf{x},t)=\prod_{j=1}^{N}p(x_j,t), \tag{4.7}$$

with

$$\int_{-\infty}^{\infty}p(x,t)dx=1.$$

Substituting this approximation into Eqs. (4.3) and (4.6) yields $\rho_k(x,t)=p(x,t)$ and

$$J_k(x,t)=J(x,t)=-D\tfrac{\partial p(x,t)}{\partial x}+\langle v(t)\rangle p(x,t)$$

for all $k=1,\ldots,N$, where

$$\langle v(t)\rangle=\frac{1}{\xi}\left[F-\kappa N\int_{-\infty}^{\infty}|x|p(x,t)dx\right]. \tag{4.8}$$

Equation (4.5) is now a closed equation of the form

$$\frac{\partial p(x,t)}{\partial t}=D\frac{\partial^2 p(x,t)}{\partial x^2}-\langle v(t)\rangle\frac{\partial p(x,t)}{\partial x}-r(x)p(x,t)+\delta(x)\int_{-\infty}^{\infty}r(x')\rho(x',t)dx. \tag{4.9}$$

B. Mean-field approximation (finite $k_{\rm on}$)

The above analysis can be extended to the case of a finite binding rate. Again select a particular bond k and introduce the marginal densities

$$\rho_{k,1}(x,t)\sum_{\mathbf{q}}\delta_{q_k,1}\left[\prod_{j=1}^{N}\int_{-\infty}^{\infty}dx_j\right]\delta(x_k-x)\rho(\mathbf{x},t,\mathbf{q}), \tag{4.10a}$$

$$\rho_{k,0}(t)\sum_{\mathbf{q}}\delta_{q_k,0}\left[\prod_{j=1}^{N}\int_{-\infty}^{\infty}dx_j\right]\rho(\mathbf{x},t,\mathbf{q}), \tag{4.10b}$$

and

$$J_k(x,t)=\sum_{\mathbf{q}}\delta_{q_k,1}\left[\prod_{j=1}^{N}\int_{-\infty}^{\infty}dx_j\right]\delta(x_k-x)J_k(\mathbf{x},t,\mathbf{q}). \tag{4.10c}$$

Summing the full CK equation (2.8) with respect to q_i and integrating with respect to x_i for all $i\neq k$ gives the following pair of equations:

$$\frac{\partial\rho_{k,1}(x,t)}{\partial t}=-\frac{\partial J_k(x,t)}{\partial x_k}-r(x)\rho_{k,1}(x,t)+\delta(x)k_{\rm on}\rho_{k,0}(t),$$

$$\frac{\partial\rho_{k,0}(t)}{\partial t}=-k_{\rm on}\rho_{k,0}(t)+\int_{-\infty}^{\infty}r(x')\rho_{k,1}(x',t)dx'.$$

Again, we do not have a closed single-bond equation because $\rho_{k,1}(x,t)$, $\rho_{k,0}(t)$, and $J_k(x,t)$ all depend on the full probability density. In particular, from Eq. (2.9)

$$J_k(x,t)=\sum_{\mathbf{q}}\delta_{q_k,1}\left[\prod_{j=1}^{N}\int_{-\infty}^{\infty}dx_j\right]\delta(x_k-x)\times\left[-D\frac{\partial\rho(\mathbf{x},t,\mathbf{q})}{\partial x_k}+v(\mathbf{x})\rho(\mathbf{x},t,\mathbf{q})\right]$$

$$=-D\frac{\partial\rho_{k,1}(x,t)}{\partial x}+\sum_{\mathbf{q}}\delta_{q_k,1}\left[\prod_{j=1}^{N}\int_{-\infty}^{\infty}dx_j\right]\delta(x_k-x)v(\mathbf{x})\rho(\mathbf{x},t,\mathbf{q}).$$

Then mean-field approximation now becomes

$$\rho(\mathbf{x},t,\mathbf{q})=\prod_{j=1}^{N}\big[q_jp(x_j,t)+(1-q_j)P_0(t)\big], \tag{4.11}$$

with

$$\int_{-\infty}^{\infty}p(x,t)dx+P_0(t)=1.$$

Substituting into Eqs. (4.10)–(4.10c) and setting $\rho_{k,1}(x.t)=p(x,t)$ and $\rho_{k,0}(t)=P_0(t)$, we obtain the closed single-bond CK equation

$$\frac{\partial p(x,t)}{\partial t}=D\frac{\partial^2 p(x,t)}{\partial x^2}-\langle v(t)\rangle\frac{\partial p(x,t)}{\partial x}-r(x)p(x,t)+\delta(x)k_{\rm on}P_0(t), \tag{4.12a}$$

$$\frac{dP_0(t)}{dt}=-k_{\rm on}P_0(t)+\int_{-\infty}^{\infty}r(x')p(x',t)dx'. \tag{4.12b}$$

C. Steady-state traction force

Although the time-dependent mean-field equation (4.12) involves a time-dependent drift $\langle v(t)\rangle$, the steady-state equations are identical to the corresponding single-bond process with a constant drift v_0, see (3.36). Imposing the normalization condition means that the time-independent version of Eq. (4.12b) is automatically satisfied. The steady-state density $p^*(x)$ for fixed v_0 can thus be determined using the analysis of Sec. III. The drift v_0 and external force F are then related according to Eq. (4.8):

$$F=F(v_0)=\xi v_0+Nf(v_0), \tag{4.13}$$

where $f(v_0)$ is the traction force

$$f(v_0)=\kappa\int_{-\infty}^{\infty}|x|p^*(x;v_0)dx. \tag{4.14}$$

The steady-state behavior of the model can now be investigated by fixing either the external drive F or the slider speed v_0. We choose the latter here, since it avoids having to solve an implicit equation for v_0 as a function of F. Our main goal is to determine how the traction force f per linkage is affected by diffusion. Dimensionless quantities are used by setting $k_{\rm off}=1$, $v=1$, and $F_b=1$. We also assume that N is sufficiently large so that the mean-field approximation holds. (In Ref. [13], numerical simulations of the full system established that the mean-field approximation can break down if N or ξ is too small, since the rupture of one bond can trigger a rupture cascade, resulting in alternating periods of stick and slip. Consequently, the joint probability distribution cannot be factorized into a product of single-bond distributions. This argument carries over when diffusion of the slider is included, since the rupturing of a bond results in a steplike change in the elastic force whose size depends on κ/ξ, whereas a Wiener process is continuous. We will ignore this complication here.)

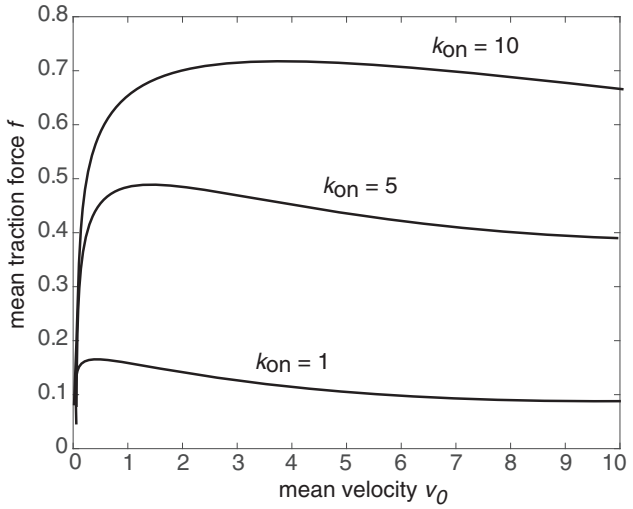

FIG. 4. Plot of the mean traction force f as a function of the mean velocity v_0 for different values of the binding rate k_{on}. Other parameters are at baseline values: $\kappa = k_{off} = F_b = 1$.

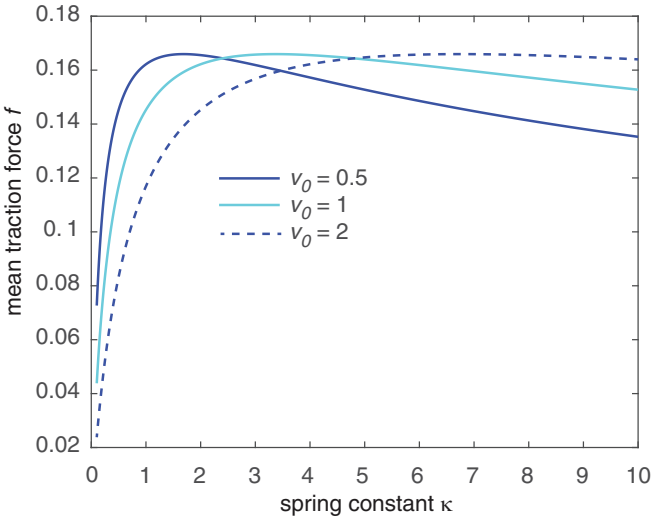

FIG. 5. Plot of the traction force f against the spring constant κ for different speeds v_0. Other parameters are at baseline values.

Within the specific context of FA dynamics, reference values for various parameters are as follows [13]: $k_{off} = 1\ s^{-1}$, $v = 10\ nm\ s^{-1}$, $F_b = 2$ pN, and $\kappa = 1 - 100$ pN nm^{-1}. Estimates of the diffusivity D or the friction coefficient ξ are difficult due to the complicated medium within which the stress fibers move, which includes multiple interactions with the actin cytoskeleton. Therefore, we will consider a range of values for D.

The steady-state traction force f for $D = 0$ can be calculated using Eqs. (3.39) and (4.14):

$$\begin{aligned} f &= \kappa \int_0^\infty x p^*(x) dx \\ &= \frac{\kappa P_0^* k_{on}}{v_0} \int_0^\infty x \exp\left[-\frac{1}{v_0}\int_0^x r(x')dx'\right]dx \\ &= \frac{P_0^* k_{on}}{v_0 \kappa} \int_0^\infty y \exp[-\gamma(y+y^3)]dy. \end{aligned}$$

Evaluating the integral along identical lines to $I_0(y)$, see Sec. III D, yields

$$\begin{aligned} I_1(\gamma) &:= \int_0^\infty y \exp[-\gamma(y+y^3)]dy \\ &= \sum_{n=0}^\infty \frac{(-1)^n}{n!} \gamma^{(2n-2)/3} \Gamma\left(\frac{n+2}{3}\right), \end{aligned} \tag{4.15}$$

and

$$f = \frac{P_0^*(\gamma) k_{on}}{v_0 \kappa} I_1(\gamma). \tag{4.16}$$

In Fig. 4 we sketch some example curves of the mean-field model, showing how the mean traction force f varies with the speed v_0. It can be seen from Fig. 4 that there is a maximum in the mean traction force at intermediate velocities. This is consistent with previous results in Ref. [13], and can be understood within the mean-field framework by noting that the average transmitted force of an engaged clutch increases monotonically with speed, while the probability of the clutch being bound decreases at higher speeds. Under the mean-field approximation, the speed at maximum traction force is independent of the number of bonds and the friction coefficient ξ. In Fig. 5 we show analogous plots of f as a function of the spring constant κ, which acts as a proxy for stiffness of the ECM.

The steady-state traction force f for $D > 0$ is given by

$$f = \kappa \int_{-\infty}^\infty |x| p^*(x) dx = \frac{\kappa}{\overline{\sigma} + T_{res}} \int_{-\infty}^\infty |x| \widetilde{\Pi}(x,0) dx.$$

Substituting for $\widetilde{\Pi}(x,0)$ and T_{res} using Eqs. (3.34) and (3.35), respectively, and evaluating the resulting integrals then yields f as a function of v_0. In Figs. 6 and Fig. 7 we plot the traction force f as a function of the mean velocity v_0 and the spring constant κ, respectively, for various values of the diffusivity D. It can be checked that in both cases the curves converge in the limit $D \to 0$. We see that diffusion has the

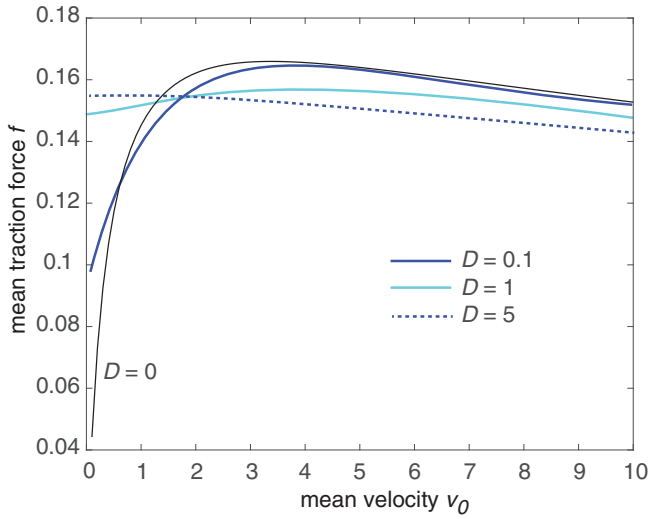

FIG. 6. Plot of steady-state traction force f as a function of the mean speed v_0 for various diffusivities D and $\kappa = k_{on} = 1$.

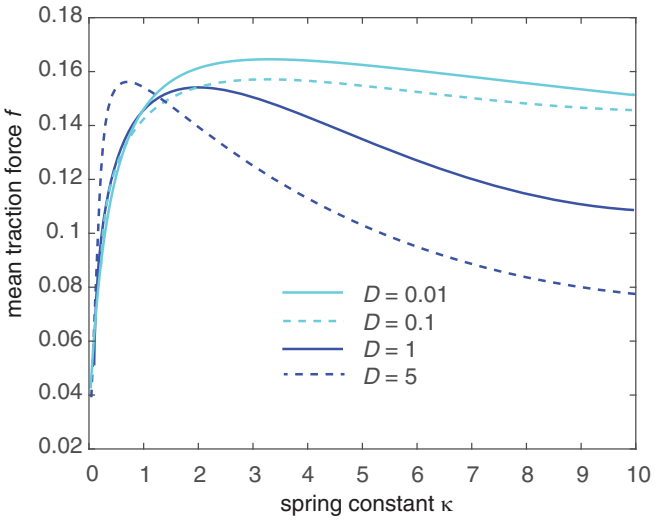

FIG. 7. Plot of steady-state traction force f as a function of the effective spring constant κ for various diffusivities D and $v_0 = k_{\rm on} = 1$.

effect of flattening the biphasic $f - v_0$ curves. On the other hand, diffusion sharpens the response with respect to κ by raising f for small κ and lowering f for large κ. In terms of the specific application to single FA dynamics, the sensitivity of the $f - \kappa$ curves to diffusion suggests that fluctuations in the driving force could play a role in the mechanosensing of ECM stiffness, as suggested in Ref. [21].

V. DISCUSSION

In this paper we used a mean-field approximation to reduce a stochastic model of sliding friction to an effective single-bond model. We then mapped the latter to an equivalent model describing an overdamped Brownian particle with spatially dependent stochastic resetting and a refractory period. This allowed us to apply recent analytical methods developed for systems with stochastic resetting, such as renewal theory and path integrals, in order to investigate the effects of diffusion on the mean traction force per bond as a function of the spring constant. In particular, we found that diffusion can sharpen the response. In terms of the application to FA dynamics, this suggests that fluctuations in the driving force could enhance the ability of the FA to act as a mechanosensor of ECM stiffness. However, a number of strong assumptions were made in the simplified model of sliding friction. First, the number N of adhesion bonds was assumed to be sufficiently large so that the mean-field approximation holds; as noted in Ref. [13], this assumption could break down in low friction regimes due to rupture cascades. Second, both positive and negative displacements of a bond were modeled in terms of the linear extension of a Hookean spring. Thus adhesive linkages were treated as slip rather than catch bonds, and geometric factors arising from the conversion of linear displacements of the slider to bond extensions were ignored. Finally, the spring constant κ of each bond was treated as a lumped parameter that included the stiffness of the ECM. A more detailed model would need to model the set of bound adhesive links in series with an ECM spring along the lines of Ref. [12].

One possible extension of the current work would be to consider other examples of collective cell adhesion. For example, cadherin-based cell-to-cell adhesions play a primary role in determining tissue structure. In addition to resisting external mechanical loads, recent evidence suggests that cadherins also couple together the actomyosin cytoskeletons of neighboring cells [37]. Hence, they are well placed to act as powerful regulators of the cytoskeleton, and to activate diverse signaling pathways in response to applied load. At the cellular level, fluctuations in the number of engaged cadherin-based linkages are coupled to the assembly and disassembly of the actomyosin cytoskeleton of connected cells. This could provide a force-dependent mechanism for consolidating certain tissue structures while supporting cellular rearrangements in other contexts. Again the stochastic breaking of a cadherin-based adhesion and subsequent rebinding could be modeled in terms of stochastic resetting with a refractory period. However, rather than modeling sliding friction, one could now investigate when a critical number of bonds are formed or broken by formulating the latter as a first passage time problem.

Finally, from a more general modeling perspective, our paper provides a concrete application of the theory of dynamical processes with stochastic resetting to cell biology. A number of other recent examples include Michaelis-Menten reaction schemes [38,39], DNA elongation and backtracking [40], and active cellular transport [41,42]. In each of these cases, analytical tools such as renewal theory can be used to investigate the behavior of the system.

APPENDIX: Eigenfunction expansion of the propgator.

An alternative approach to evaluating $\Pi(x,t)$ is to consider an eigenfunction expansion of the propagator. Suppose that $\Delta r(x)$ acts like a confining potential [$\Delta r(x) \to \infty$ for $x \to \pm\infty$], so there exists a complete set of orthonormal eigenfunctions $\phi_n(x)$, $n = 0, 1, \ldots$, with

$$\left[-D\frac{\partial^2}{\partial x^2} + \Delta r(x)\right]\phi_n(x) = E_n\phi_n(x) \tag{A1}$$

such that

$$\int_{-\infty}^{\infty} \phi_n(x)\phi_m(x)dx = \delta_{n,m}.$$

Then

$$\mathcal{G}_r(x, -it|x_0, 0) = \sum_{n\geqslant 0} e^{-E_n t}\phi_n(x_0)\phi_n(x). \tag{A2}$$

If we now substitute the eigenfunction expansion (A2) into Eq. (3.30) and take the Laplace transform, we obtain the series expansion

$$\widetilde{\Pi}(x,s) = e^{xv_0/2D}\sum_{n\geqslant 0}\frac{\phi_n(0)\phi_n(x)}{s + r_0 + v_0^2/4D + E_n}. \tag{A3}$$

Substituting into Eq. (3.13) gives

$$p^*(x) = e^{xv_0/2D}\lim_{s\to 0}\frac{s\sum_{n\geqslant 0}\frac{\phi_n(0)\phi_n(x)}{s+r_0+v_0^2/4D+E_n}}{1-\widetilde{\psi}(s)\sum_{n\geqslant 0}\frac{\Gamma_n\phi_n(0)}{s+r_0+v_0^2/4D+E_n}},$$

where

$$\Gamma_n = \int_0^\infty \Delta r(y) e^{yv_0/2D} \phi_n(y) dy. \tag{A4}$$

Applying L'Hopital's rule and the normalization $\widetilde{F}(0) = 1$ yields the result

$$p^*(x) = \frac{e^{xv_0/2D} \sum_{n\geqslant 0} \frac{\phi_n(0)\phi_n(x)}{v_0^2/4D + r_0 + E_n}}{1 + \overline{\sigma} + \sum_{n\geqslant 0} \frac{\Gamma_n \phi_n(0)}{(v_0^2/4D + r_0 + E_n)^2}}. \tag{A5}$$

Equation (A5) yields an explicit series expansion of the steady-state density $p^*(x)$. However, this is predicated on knowing the eigenfunctions and eigenvalues of the Hamiltonian operator $\widehat{H}$. Again, there are only a few potentials for which exact results are known. In the particular case of a harmonic potential, $\Delta r(x) = \alpha x^2$, the eigenvalues are

$$E_n = \left(n + \frac{1}{2}\right)\sqrt{4D\alpha}, \tag{A6}$$

and the normalized eigenfunctions are

$$\phi_n(x) = \frac{1}{\sqrt{2^n n! \sqrt{\pi}}} \left(\sqrt{\frac{\alpha}{D}}\right)^{1/4} H_n[(\alpha/D)^{1/4} x] e^{-\sqrt{\alpha/D}x^2/2}, \tag{A7}$$

with $H_n(x)$ the Hermite polynomial of integer order n. However, it is simpler to use the explicit expressions given by Eqs. (3.30) and (3.33). Although the eigenvalue problem for the nonanalytic, symmetrized exponential potential $r_0 e^{\kappa|x|/F_b}$ has also been analyzed [43], the numerical evaluation of the eigenvalues is rather delicate and not useful for our purposes. (The eigenfunctions are given by modified Bessel functions K_ν and the eigenvalues are determined from the equation $K_{2i\sqrt{E_n/D(\kappa/F_b)^2}}[2\sqrt{r_0/D(\kappa/F_b)^2}] = 0$.)

[1] J. T. Parsons, A. R. Horwitz, and M. A. Schwartz, Cell adhesion: Integrating cytoskeletal dynamics and cellular tension, Nat. Rev. Mol. Cell Biol. **11**, 633 (2010).

[2] U. S. Schwarz and S. A. Safran, Physics of adherent cells, Rev. Mod. Phys. **85**, 1327 (2013).

[3] M. Vicente-Manzanares, C. K. Choi, and A. R. Horwitz, Integrins in cell migration–the actin connection, J. Cell Sci. **122**, 199 (2009).

[4] T. J. Mitchison and M. W. Kirschner, Cytoskeletal dynamics and nerve growth, Neuron **1**, 761 (1988).

[5] C. H. Lin and P. Forscher, Growth cone advance is inversely proportional to retrograde f-actin flow, Neuron **14**, 763 (1995).

[6] C. Jurado, J. R. Haserick, and J. Lee, Slipping or gripping? Fluorescent speckle microscopy in fish keratocytes reveals two different mechanisms for generating a retrograde flow of actin, Mol. Biol. Cell **16**, 507 (2005).

[7] W. H. Guo and Y. L. Wang, Retrograde fluxes of focal adhesion proteins in response to cell migration and mechanical signals, Mol. Biol. Cell **18**, 4519 (2007).

[8] G. Giannone, R. M. Mege, and O. Thoumine, Multi-level molecular clutches in motile cell processes, Trends Cell Biol. **19**, 475 (2009).

[9] A. Schallamach, A theory of dynamic rubber friction, Wear **6**, 375 (1963).

[10] A. E. Filippov, J. Klafter J, and M. Urbakh, Friction Through Dynamical Formation and Rupture of Molecular Bonds, Phys. Rev. Lett. **92**, 135503 (2004).

[11] M. Srinivasan and S. Walcott, Binding site models for friction due to the formation and rupture of bonds: State-function formalism, force-velocity relations, response to slip velocity transients, and slip stability, Phys. Rev. E **80**, 046124 (2009).

[12] C. E. Chan and D. J. Odde, Traction dynamics of filopodia on compliant substrates, Science **322**, 1687 (2008).

[13] B. Sabass and U. S. Schwarz, Modeling cytoskeletal flow over adhesion sites: Competition between stochastic bond dynamics and intracellular relaxation, J. Phys. Condens. Matter. **22**, 194112 (2010).

[14] Y. Li, P. Bhimalapuram, and A. R. Dinner, Model for how retrograde actin flow regulates adhesion traction stresses, J. Phys. Condens. Matter. **22**, 194113 (2010).

[15] P. Sens, Rigidity sensing by stochastic sliding friction, Europhys. Lett. **104**, 38003 (2013).

[16] B. L. Bangasser, S. S. Rosenfeld, and D. J. Odde, Determinants of maximal force transmission in a motor-clutch model of cell traction in a compliant microenvironment, Biophys. J. **105**, 581 (2013).

[17] P. S. De and R. De, Stick-slip dynamics of migrating cells on viscoelastic substrates, Phys. Rev. E **100**, 012409 (2019).

[18] B. Ladoux and A. Nicolas, Physically based principles of cell adhesion mechanosensitivity in tissues, Rep. Prog. Phys. **75**, 116601 (2012).

[19] J. Z Kechagia, J. Ivaska, and P. Roca-Cusachs, Integrins as biomechanical sensors of the microenvironment, Nature Rev. Mol. Cel. Biol. **20**, 457 (2019).

[20] C. M. Lo, H. B. Wang, M. Dembo, and Y. L. Wang, Cell movement is guided by the rigidity of the substrate, Biophys. J. **79**, 144 (2000).

[21] S. V. Plotnikov and C. M. Waterman, Guiding cell migration by tugging, Curr. Opin. Cell Biol. **25**, 619 (2013).

[22] R. Sunyer and X. Trepat, Durotaxis, Curr. Biol. **30**, R383 (2020).

[23] S. V. Plotnikov, A. M. Pasapera, B. Sabass, and C. M. Waterman, Force fluctuations within focal adhesions mediate ECM- rigidity sensing to guide directed cell migration, Cell **151**, 1513 (2012).

[24] M. R. Evans and S. N. Majumdar, Diffusion with Stochastic Resetting, Phys. Rev. Lett. **106**, 160601 (2011).

[25] M. R. Evans and S. N. Majumdar, Diffusion with optimal resetting, J. Phys. A Math. Theor. **44**, 435001 (2011).

[26] M. R. Evans and S. N. Majumdar, Diffusion with resetting in arbitrary spatial dimension, J. Phys. A: Math. Theor. **47**, 285001 (2014).

[27] M. R. Evans, S. N. Majumdar, and G. Schehr, Stochastic resetting and applications, J. Phys. A **53**, 193001 (2020).

[28] A. Pal, Diffusion in a potential landscape with stochastic resetting, Phys. Rev. E **91**, 012113 (2015).

[29] E. Roldan and S. Gupta, Path-integral formalism for stochastic resetting: Exactly solved examples and shortcuts to confinement, Phys. Rev. E **96**, 022130 (2017).

[30] M. R. Evans and S. N. Majumdar, Effects of refractory period on stochastic resetting, J. Phys. A: Math. Theor. **52**, 01LT01 (2019).

[31] G. I. Bell, Models for specific adhesion of cells to cells, Science **200**, 618 (1978).

[32] E. Evans and K. Ritchie, Dynamic strength of molecular adhesion bonds, Biophys. J. **72**, 1541 (1997).

[33] P. C. Bressloff, *Stochastic Processes in Cell biology* (Springer, New York, 2014).

[34] More precisely, in the analysis of Ref. [13] the displacements are restricted to be positive, $x_i \geqslant 0$ for all $i = 1, \ldots, N$. The term $A_i(\mathbf{x}, , t, \mathbf{q})$ multiplying $\delta(x_i)$ in Eq. (2.8) is modified accordingly:

$$A_i = (1 - q_i) \int_0^\infty r(x_i') \, \rho(\mathbf{x}, t, \mathbf{q})|_{(x_i, q_i) = (x_i', 1)} dx_i'$$

$$+ \, q_i [k_{\rm on} \rho(\mathbf{x}, t, \mathbf{q})|_{q_i = 0} - J(\mathbf{x}, t, \mathbf{q}),$$

with flux $J(\mathbf{x}, t, \mathbf{q}) = v(\mathbf{x}) \rho(\mathbf{x}, t, \mathbf{q})$. The inclusion of the flux term ensures conservation of flux at each boundary $x_j = 0$.

[35] R. P. Feynman and A. R. Hibbs, *Quantum Mechanics and Path Integrals* (McGraw–Hill, New York, 2010).

[36] L. S. Schulman, *Techniques and Applications of Path Integration* (John Wiley Sons, Chichester, UK, 1981).

[37] B. D. Hoffman and A. S. Yap, Towards a dynamic understanding of cadherin-based mechanobiology, Trends Cell Biol. **25**, 803 (2015).

[38] S. Reuveni, M. Urbakh, and J. Klafter, Role of substrate unbinding in Michaelis-Menten enzymatic reactions, Proc. Natl Acad. Sci. USA **111**, 4391 (2014).

[39] T. Rothart, S. Reuveni, and M. Urbakh, Michaelis-Menten reaction scheme as a unified approach towards the optimal restart problem, Phys. Rev. E **92**, 060101 (2015).

[40] E. Roldan, A. Lisica, D. Sanchez-Taltavull, and S. W. Grill, Stochastic resetting in backtrack recovery by RNA polymerases, Phys. Rev. E **93**, 062411 (2016).

[41] P. C. Bressloff, Directed intermittent search with stochastic resetting, J. Phys. A **53**, 105001 (2020).

[42] P. C. Bressloff, Modeling active cellular transport as a directed search process with stochastic resetting and delays, J. Phys. A **53**, 355001 (2020).

[43] M. Znojil, Symmetrized exponential oscillator, Mod. Phys. Lett. A **31**, 1650195 (2016).